

Direct observation of proton emission in ^{11}Be

Y. Ayyad,^{1,2,*} B. Olaizola,³ W. Mittig,^{2,4} G. Potel,¹ V. Zelevinsky,^{1,2,4} M. Horoi,⁵ S. Beceiro-Novo,⁴ M. Alcorta,³ C. Andreoiu,⁶ T. Ahn,⁷ M. Anholm,^{3,8} L. Atar,⁹ A. Babu,³ D. Bazin,^{2,4} N. Bernier,^{3,10} S. S. Bhattacharjee,³ M. Bowry,³ R. Caballero-Folch,³ M. Cortesi,² C. Dalitz,¹¹ E. Dunling,^{3,12} A.B. Garnsworthy,³ M. Holl,^{3,13} B. Kootte,^{3,8} K. G. Leach,¹⁴ J.S. Randhawa,² Y. Saito,^{3,10} C. Santamaria,¹⁵ P. Šiurytė,^{3,16} C.E. Svensson,⁹ R. Umashankar,³ N. Watwood,² and D. Yates^{3,10}

¹Facility for Rare Isotope Beams, Michigan State University, East Lansing, Michigan 48824, USA

²National Superconducting Cyclotron Laboratory, Michigan State University, East Lansing, Michigan 48824, USA

³TRIUMF, 4004 Wesbrook Mall, Vancouver, British Columbia V6T 2A3, Canada

⁴Department of Physics and Astronomy, Michigan State University, East Lansing, MI 48824, U.S.A.

⁵Department of Physics, Central Michigan University, Mount Pleasant, MI 48859, USA

⁶Department of Chemistry, Simon Fraser University, Burnaby, BC V5A 1S6, Canada

⁷Department of Physics, University of Notre Dame, Notre Dame, Indiana, 46556, USA

⁸Department of Physics and Astronomy, University of Manitoba, Winnipeg, Manitoba, R3T 2N2, Canada

⁹Department of Physics, University of Guelph, Guelph, Ontario N1G 2W1, Canada

¹⁰Department of Physics and Astronomy, University of British Columbia, Vancouver, BC, V6T 1Z4, Canada

¹¹Niederrhein University of Applied Sciences, Institute for Pattern Recognition

Reinartzstr. 49, 47805 Krefeld, Germany

¹²Department of Physics, University of York, Heslington, York YO10 5DD, United Kingdom

¹³Department of Astronomy and Physics, Saint Marys University, Halifax, Nova Scotia B3H 3C3, Canada

¹⁴Department of Physics, Colorado School of Mines, Golden, Colorado 80401, USA

¹⁵Nuclear Science Division, Lawrence Berkeley National Laboratory, Berkeley, California 94720, USA

¹⁶Department of Physics, University of Surrey, Guildford, Surrey, GU2 7XH, United Kingdom

(Dated: February 19, 2022)

The elusive β^-p^+ decay was observed in ^{11}Be by directly measuring the emitted protons and their energy distribution for the first time with the prototype Active Target Time Projection Chamber (pAT-TPC) in an experiment performed at ISAC-TRIUMF. The measured β^-p^+ branching ratio is orders of magnitude larger than any previous theoretical model predicted. This can be explained by the presence of a narrow resonance in ^{11}B above the proton separation energy.

Keywords: ^{11}Be , ^{11}B , β -delayed particle emission, β^-p^+ , proton emission, halo nucleus

It would seem, *a priori*, that β^- -decay and proton emission are incompatible processes in a neutron-rich nucleus. The β^- decay moves isotopes north-west in the nuclear chart, towards the valley of stability and more bound systems, while the proton emission takes it south, becoming a less stable system. This process, called β^- -delayed proton emission (β^-p^+), is energetically forbidden in all but some nuclei for which their neutron separation energy is $S_n < 782$ keV [1]. Only a handful of $A \leq 31$ nuclei that fulfil this condition have been observed, of which the most promising candidate is $^{11}\text{Be} \rightarrow ^{10}\text{Be} + p^+ + \beta^-$.

Nuclei approaching the nuclear drip lines have large Q_β values available and decay into nuclei with low particle binding energy. This opens an energy window where different β -delayed particle emission channels are allowed [2]. ^{11}Be , which is the last bound odd beryllium isotope, has several of them energetically available: $\beta\alpha$ ($Q_{\beta\alpha}=2845.2(2)$ keV, $b_\alpha=3.30(10)\%$ [3]), βt ($Q_{\beta t}=285.7(2)$ keV, not observed), β^-p^+ ($Q_{\beta p}=280.7(3)$ keV, $b_p=8.3(9) \cdot 10^{-6}$, indirectly observed [4]) and βn ($Q_{\beta n}=55.1(5)$ keV, not observed).

This low neutron binding energy allows for the counterintuitive β^-p^+ decay to happen. In nuclei like ^{11}Be , called halo nuclei, the last neutron is so weakly bound that it orbits far from an inert core [5–7]. The β^-p^+ decay mechanism has been modeled as a decay of the halo neutron into a proton that is either in a high-energy resonant state above its separation energy or directly in the continuum, free to be emitted [8]. This is similar to the β -delayed deuterium emission in the two-neutron halo nucleus ^{11}Li . When one of the neutrons decays into a proton, it binds to the other forming a deuteron coupled to the continuum [9].

Riisager and collaborators performed experiments at ISOLDE to indirectly observe the $^{11}\text{Be} \rightarrow ^{10}\text{Be}$ decay [4, 12, 13]. They implanted ^{11}Be ($T_{1/2}=13.8$ s) in a catcher. Using accelerated mass spectroscopy, they measured the amount of ^{10}Be ($T_{1/2} = 1.5 \cdot 10^6$ years) in the samples, obtaining $b_p = 8.3(9) \cdot 10^{-6}$. Theoretical predictions using the ^{11}B nuclear structure suggest that the β^-p^+ branch should have been orders of magnitude lower than observed [1, 8, 12].

There are two possible explanations for this discrepancy. The β^-p^+ decay could populate some unobserved resonance in ^{11}B , changing the available phase space and enhancing the decay, or there could be additional, unac-

* Corresponding author. ayyadlim@frib.msu.edu

counted for decay channels contributing to the total $^{11}\text{Be} \rightarrow ^{10}\text{Be}$ decay. Recently, it was suggested in Refs. [14, 15] that the halo neutron in ^{11}Be is so weakly bound that it could decay into a particle of the dark sector, thus creating a ^{10}Be nucleus and an undetectable dark particle. The experiment in Ref. [4] measured the total branching ratio of the $^{11}\text{Be} \rightarrow ^{10}\text{Be}$ decay, not the individual branching of the β^-p^+ and other hypothetical dark decay channels. The implications of this alternative dark decay in ^{11}Be will be discussed at length in the other publication reporting results of this experiment [16].

The aim of our experiment was to directly measure the β^-p^+ decay in ^{11}Be and unambiguously assign a branching ratio to that specific decay channel. By directly observing the emitted protons and measuring their energy distribution, important information can be extracted about ^{11}B nuclear structure and the β^-p^+ decay mechanism.

In order to efficiently detect and identify every particle emitted in the β -decay of ^{11}Be , specially protons of ~ 200 keV of energy [4, 8], the experiment was performed with the prototype Active Target Time Projection Chamber (pAT-TPC) [17]. This device allows for efficient and high-resolution measurement of very low energy particles. The pAT-TPC consists of a cylindrical gaseous volume of 50 cm length with 12 cm radius with a detection plane composed of a dual micropattern gas detector (Micromegas [18] coupled to a Multi-layer Thick Gas Electron Multiplier [19]). An electric field is applied along the beam axis between the cathode end and the detection plane. Ionization electrons released when a charged particle is crossing the gaseous volume are drifted to the segmented pad plane. There they are multiplied and collected in the Micromegas readout pads. The drift time and the energy loss rate are recorded by each pad individually. With this information and the centroids of the pads, the characteristic energy loss curve of each particle and their tracks can be reconstructed. Each particle track was analyzed independently using a sophisticated clustering algorithm [20]. Further information about the pAT-TPC can be found in Refs. [17, 21, 22].

The ^{11}Be isotopes were produced by a 480-MeV proton beam (9.8 μA of intensity) delivered by the TRIUMF main cyclotron [23] impinging on a uranium carbide (UC_x) target. The TRIUMF Resonant Ionization Laser Ion Source [24] selectively ionized Be isotopes to a 1^+ state. After separation of $A/q=11$, particles were further stripped to a $q=2^+$ state and re-accelerated to ~ 390 A keV. The beam intensity was attenuated to $\sim 10^5$ particles per second to reduce downtime. The experiment was run in a cycled mode: ions were implanted for 1 s, the charge carriers produced during the implantation were evacuated for 0.5 s and finally 7 s were used to observe ^{11}Be decay. The beam energy was selected to stop the ^{11}Be at the center of the pAT-TPC. The ions were expected to neutralize and undergo minimal Brownian mo-

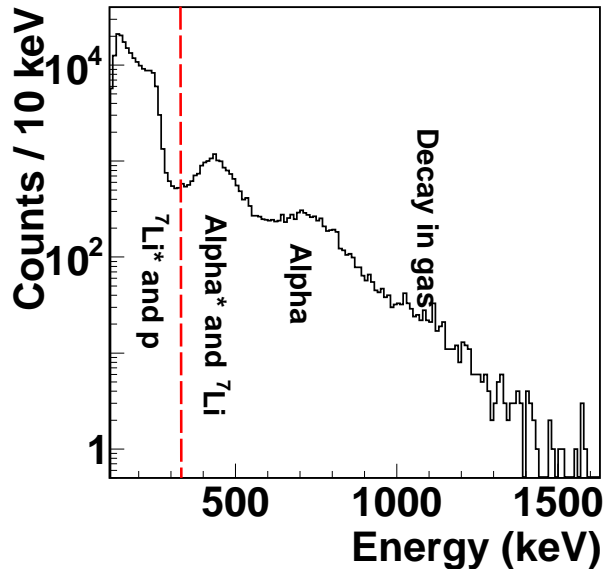


FIG. 1. ^{11}Be β^- -decay energy spectrum measured with the pAT-TPC. The dashed line separates both energy regions defined by the *low-level* and *high-level* triggers. Alpha* refers to the ^4He emitted together with $^7\text{Li}^*$.

tion. However, most of the ^{11}Be drifted to the cathode where they decayed. The response of the pAT-TPC to low-energy protons was determined by injecting protons in the detector. A molecular OH^+ beam was extracted from the Off-Line Ion Source and accelerated before impacting a thin foil to break up the molecule. The p^+ was then further accelerated to 220 keV/A. Protons entered the TPC gas volume with $E = 198$ keV, as inferred from energy loss parameterizations. The energy resolution of the detector, which amounts to about 15 keV (FWHM) was obtained by integrating the energy loss curve for each proton event to determine the total deposited charge.

The detector was filled with 60 torr of $^4\text{He}+\text{CO}_2$ (90-10%) gas mixture to stop 200 keV protons within ~ 10 cm. Due to the extremely low branching ratio expected for the β^-p^+ channel, two different triggers, *low*- and *high*-level, were used to separate regions of interest in the energy spectrum: 20-300 keV and 300-1500 keV, respectively. The latter was downscaled by a factor of 64 to reduce the triggers of the $\beta\alpha$ decay.

Figure 1 shows the total energy spectrum of charged particles emitted following the ^{11}Be β -decay. The vertical dashed line indicates the separation between trigger windows. One of the products of the decay into $^7\text{Li} + ^4\text{He}$ and $^7\text{Li}^* + ^4\text{He}$, coming from the cathode of the detector, was identified on an event-by-event basis. In addition, decays in the gas, in which both products were detected simultaneously, ($\sim 10\%$ of the total) were also measured (1200 keV).

The identification of protons in the region of interest,

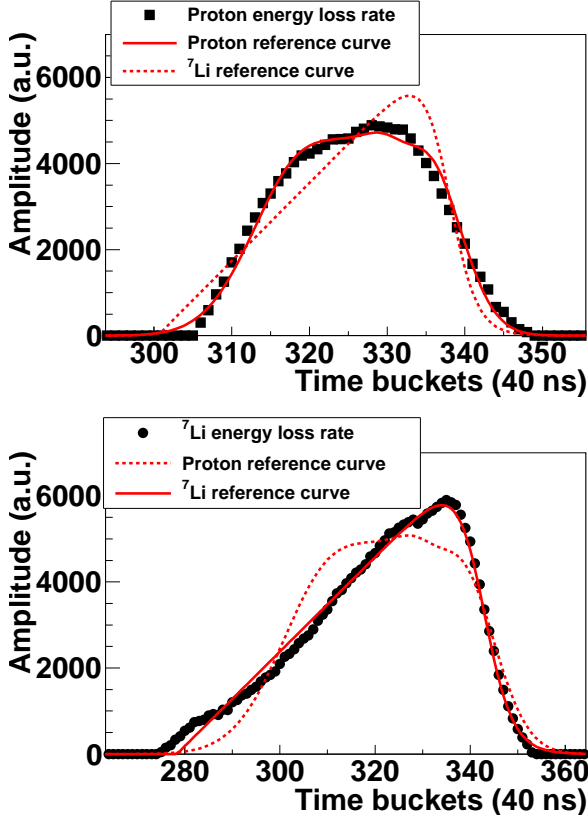


FIG. 2. (Upper panel) Experimental energy loss for protons (squares) compared to the reference curves (solid and dotted lines for protons and ${}^7\text{Li}$, respectively). The calculated χ^2 are 111 (proton reference curve) and 1034 (${}^7\text{Li}$ one). (Lower panel) Same as upper panel but for ${}^7\text{Li}^*$ (dotted and solid lines for ${}^7\text{Li}$ and protons, respectively). In this case, the calculated χ^2 is 1890 (proton) and 190 (${}^7\text{Li}$).

which is dominated by ${}^7\text{Li}^*$, was performed using the characteristic energy loss distribution. An analytical energy loss curve fit to experimental proton and ${}^7\text{Li}$ energy loss curves was used to perform a χ^2 -test for every particle track. These reference curves determined experimentally are shown in Fig. 2 for a β^-p^+ decay (upper panel) and a ${}^7\text{Li}^*+{}^4\text{He}$ decay (lower panel) event. In these events, both the proton and ${}^7\text{Li}^*$ are emitted from the cathode of the detector. The experimental energy loss curves of each event (square for protons and dots for ${}^7\text{Li}^*$) were compared to both reference curves using an objective function containing the amplitude (energy loss) per unit time (time bucket). Since the reference curves were determined at a fixed angle and energy, they were shaped and re-normalized to take into account the energy-range of the particle, its angle of emission and the starting time bucket of the event. In each step of the algorithm, the objective function is evaluated, selecting the curve that minimizes the χ^2 .

The results of the minimization process, in terms of χ^2 ,

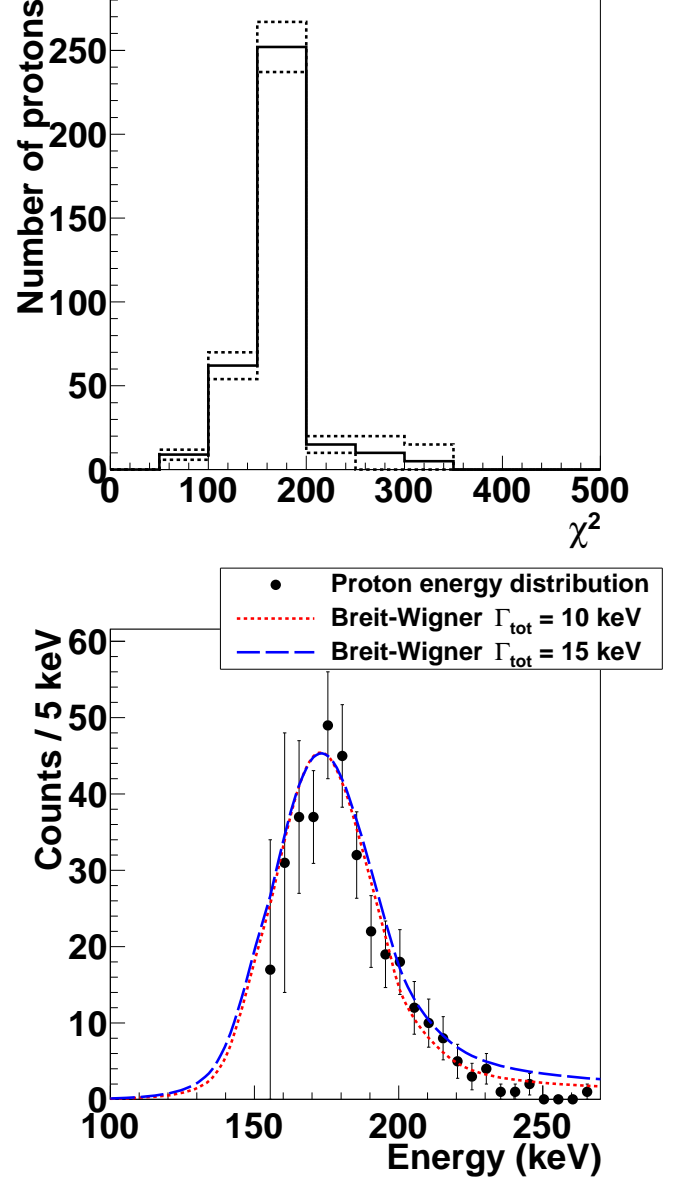


FIG. 3. (Upper panel) Number of identified protons as a function of the χ^2 range (solid line). The dashed line refers to the uncertainty limits. (Lower panel) Energy distribution of β -delayed protons ($\chi^2 < 200$) emitted from ${}^{11}\text{Be}$ (solid dots) compared to a Breit-Wigner distribution.

have also been validated by scrutiny. The β^-p^+ decay candidates, 391 in total, were inspected and found to be similar to the one shown in the upper panel of Fig. 2.

Background and misidentification of events in the energy spectrum were evaluated by analyzing the distribution as a function of χ^2 value (not normalized), as shown

in Fig. 3. Below a χ^2 value of 200¹, the energy spectrum (solid dots in the lower panel) exhibits a clear peak that is in excellent agreement with a Breit-Wigner distribution with two contributions: protons emitted from the cathode with 178(20) keV, and 10% of decays in gas with 196 keV (178 keV plus 18 keV from the ¹⁰Be recoil), respectively, both with a width of 12(5) keV. The proton penetrability as a function of the energy was also taken into account. The sharp energy distribution clearly indicates that the β^-p^+ decay from ¹¹Be proceeds through an unobserved resonance in ¹¹B. Based on the Q_β and the proton plus recoil energies (the electron screening term is negligible for Be), the resonance is predicted at an energy of 11425(20) keV. From the proton energy distribution, and taking into account the detector energy resolution, the width of the resonance is $\Gamma = 12(5)$ keV. The branching ratio for the β^-p^+ channel was obtained relative to the well known $\beta\alpha$ one, $b_\alpha = 3.30(10)\%$ [3]. The result is $1.3(3) \cdot 10^{-5}$, in agreement with the previous indirect measurement [4]. The measured branching ratio and resonance energy yields a very small $\log(ft) = 4.8(4)$, which suggests a strongly allowed β decay. From the β decay selection rule of the $J^\pi = 1/2^+$ ¹¹Be gs.s, we can assume $\Delta J = 0, 1$ and no change in parity, therefore we propose $J^\pi = (1/2, 3/2^+)$ for the newly found resonance.

We evaluated the probability of the direct “democratic” decay (simultaneous emission of the proton and β^-) when there are four particles in the final state: electron (\mathbf{p}_e , ϵ_e), electron antineutrino (\mathbf{p}_ν , ϵ_ν), proton (\mathbf{p} , E) and the final nucleus (\mathbf{P} , $E \sim 0$). The release of kinetic energy is 11506-11228=278 keV so that for the electron $p_e R \sim (1/400)(R/\text{fm})$, i.e. always small even for halo nuclei with $R \sim 10$ fm (even smaller for the antineutrino). The density of final states for free particles can be estimated, with the normalization to the unit volume, as:

$$\rho(E) = (2\pi\hbar)^3 \delta(\mathbf{P} + \mathbf{p} + \mathbf{p}_e + \mathbf{p}_\nu) \times \delta(\Delta - E - \epsilon_e - \epsilon_\nu) \frac{d^3 P d^3 p d^3 p_e d^3 p_\nu}{(2\pi\hbar)^{12}},$$

The probability of the decay is:

$$dw(E) = \frac{2\pi}{\hbar} G^2 |\mathcal{M}|^2 \frac{p_\nu^2 d\mathbf{p}_\nu p_e^2 d\mathbf{p}_e p^2 d\mathbf{p}}{(2\pi\hbar)^9} \times dp_e dp_\nu \frac{dp}{dE} dE \delta(X - \epsilon_e - \epsilon_\nu),$$

where X is the total energy of the electron and antineutrino including $m_e c^2$, and \mathcal{M} is the dimensionless sum of the Fermi and Gamow-Teller nuclear matrix elements depending on the halo wave-function.

The integration can be performed exactly:

$$dw(E) = \frac{1}{4\pi^5} \frac{m^5 c^4}{\hbar^{10}} G^2 |\mathcal{M}|^2 f_0(x) p^2 dp, \quad (1)$$

where $x = X/mc^2$ and:

$$f_0(x) = \frac{1}{5} \left(\frac{1}{6} x^4 - \frac{3}{4} x^2 - \frac{2}{3} \right) \times \sqrt{x^2 - 1} + \frac{1}{4} x \ln \left(x + \sqrt{x^2 - 1} \right).$$

The inverse lifetime follows as (M is the nucleon mass)

$$\tau^{-1} = \frac{\sqrt{2}}{4\pi^5} \frac{M^{3/2} m^{13/2} c^7}{\hbar^{10}} G^2 \int_0^\Omega d\epsilon \sqrt{\epsilon} f_0(x) |\mathcal{M}|^2. \quad (2)$$

For calculating the matrix element, we use the analytic form of the neutron halo wave-function [26] and the Coulomb proton wave-function in the field of the charge $Z = 5$. The result for the half-life summing the Fermi and Gamow-Teller contributions is $\tau_{1/2} \sim 2.2 \cdot 10^{10}$ s which corresponds to a branching ratio $6.3 \cdot 10^{-10}$ for the democratic decay, in glaring contrast with the experimental result.

We also estimated the β -decay rate of ¹¹Be into a proton-emitting resonance of ¹¹B, using a simple model to compute the overlap $\mathcal{O} = \langle \phi_n | \phi_p \rangle$ between the halo neutron $\phi_n(2s_{1/2})$ in ¹¹Be and the final single-proton resonance $\phi_p(2s_{1/2})$ of ¹¹B, as well as the width Γ_p of the resonance. Both states are calculated making use of Woods-Saxon potentials similar to those used in [8], complemented with the Coulomb interaction in the proton case. Setting the resonance energy at the experimental value, the overlap and the width are found to be $\mathcal{O} = 0.53$ and $\Gamma_p = 44$ keV, respectively. Within this model, we can also give a rough estimate of the spectroscopic factor $S(^{11}\text{B})$ of the ¹¹B resonance using the expression $\gamma_p = S(^{11}\text{B})\Gamma_p$, where γ_p is the experimental proton emission width. We obtained $S(^{11}\text{B}) \approx 0.34$, suggesting that the newly observed ¹¹B resonance has a sizable single-proton content.

The corresponding partial lifetime $t_{1/2}^p$ can be estimated by integrating the Gamow-Teller strength over a Lorentzian distribution characterizing the energy spreading of the resonance, with the experimental centroid and width. We assume that the spectroscopic factor of the halo neutron of the ¹¹Be ground state is ≈ 1 [27], and that the initial and final isospins are $T_i = 3/2$ and $T_f = 1/2$. This results in a pure Gamow-Teller transition, with $\langle F \rangle = 0$ and $g_A^2 \langle GT \rangle^2 = 0.15$. With the values of the overlap \mathcal{O} and the spectroscopic factor $S(^{11}\text{B})$ estimated above, we obtain $t_{1/2}^p = 1.7 \times 10^6$ s, and $b_p = 8.0 \times 10^{-6}$.

In summary, we have performed the first direct observation of a β^-p^+ decay. This new result is in agreement with the previous indirect measurement [4]. The

¹ This value was chosen based on a correlation matrix showing the χ^2 obtained comparing both reference curves.

use of the pAT-TPC also allowed for a precise measurement of the emitted proton energy, which in turn clarified that the decay proceeds sequentially through a narrow resonance [$E = 11425(20)$ keV, $\Gamma = 12(5)$ keV, $J^\pi = (1/2, 3/2^+)$] in ^{11}B . This resonance, unobserved yet, also explains why the branching ratio is orders of magnitude larger than previous theoretical models predicted. Calculations including this new result can reproduce the measured branching ratio. In contrast, when a democratic decay is considered, the result is orders of magnitude lower than observed.

The authors would like to thank the beam operators at ISAC-TRIUMF for their effort. They set up a new proton beam of the exact needed energy in a very short time that turned out to be crucial for the successful outcome of the experiment. TRIUMF receives funding through a contribution agreement through the National Research Council Canada. This work was supported by the Natural Sciences and Engineering Research Council of Canada, by the DOE Office of Science (grant DE-SC-0017649, and FRIB Theory Alliance award DE-SC0013617) and the by the U.S. National Science Foundation (NSF) under Cooperative Agreement No. PHY-1565546.

[1] D. Baye and E. Tursunov, *Physics Letters B* **696**, 464 (2011).
 [2] M. J. G. Borge, *Physica Scripta* **T152**, 014013 (2013).
 [3] J. Refsgaard, J. Büscher, A. Arokiaraj, H. O. U. Fynbo, R. Raabe, and K. Riisager, *Phys. Rev. C* **99**, 044316 (2019).
 [4] K. Riisager, O. Forstner, M. Borge, J. Briz, M. Carmona-Gallardo, L. Fraile, H. Fynbo, T. Giles, A. Gotthberg, A. Heinz, J. Johansen, B. Jonson, J. Kurcewicz, M. Lund, T. Nilsson, G. Nyman, E. Rapisarda, P. Steier, O. Tengblad, R. Thies, and S. Winkler, *Physics Letters B* **732**, 305 (2014).
 [5] I. Tanihata, *Journal of Physics G: Nuclear and Particle Physics* **22**, 187 (1996).
 [6] J. Al-Khalili, “An introduction to halo nuclei,” in *The Euroschool Lectures on Physics with Exotic Beams, Vol. I*, edited by J. Al-Khalili and E. Roeckl (Springer Berlin Heidelberg, Berlin, Heidelberg, 2004) pp. 77–112.
 [7] I. Tanihata, H. Savajols, and R. Kanungo, *Progress in Particle and Nuclear Physics* **68**, 215 (2013).
 [8] K. Riisager, *Nuclear Physics A* **925**, 112 (2014).
 [9] R. Raabe, A. Andreyev, M. J. G. Borge, L. Buchmann, P. Capel, H. O. U. Fynbo, M. Huyse, R. Kanungo, T. Kirchner, C. Mattoon, A. C. Morton, I. Mukha, J. Pearson, J. Ponsaers, J. J. Ressler, K. Riisager, C. Ruiz, G. Ruprecht, F. Sarazin,

O. Tengblad, P. Van Duppen, and P. Walden, *Phys. Rev. Lett.* **101**, 212501 (2008).
 [10] I. Tanihata, T. Kobayashi, O. Yamakawa, S. Shimoura, K. Ekuni, K. Sugimoto, N. Takahashi, T. Shimoda, and H. Sato, *Physics Letters B* **206**, 592 (1988).
 [11] M. Fukuda, T. Ichihara, N. Inabe, T. Kubo, H. Kumagai, T. Nakagawa, Y. Yano, I. Tanihata, M. Adachi, K. Asahi, M. Kouguchi, M. Ishihara, H. Sagawa, and S. Shimoura, *Physics Letters B* **268**, 339 (1991).
 [12] M. J. G. Borge, L. M. Fraile, H. O. U. Fynbo, B. Jonson, O. S. Kirsebom, T. Nilsson, G. Nyman, G. Possnert, K. Riisager, and O. Tengblad, *Journal of Physics G: Nuclear and Particle Physics* **40**, 035109 (2013).
 [13] K. Riisager, *Few-Body Systems* **58**, 106 (2017).
 [14] B. Fornal and B. Grinstein, *Phys. Rev. Lett.* **120**, 191801 (2018).
 [15] M. Pfützner and K. Riisager, *Phys. Rev. C* **97**, 042501 (2018).
 [16] B. Olaizola, Y. Ayyad, W. Mittig, and *et al.*, Unpublished (2019).
 [17] D. Suzuki, M. Ford, D. Bazin, W. Mittig, W. Lynch, T. Ahn, S. Aune, E. Galyaev, A. Fritsch, J. Gilbert, F. Montes, A. Shore, J. Yurkon, J. Kolata, J. Browne, A. Howard, A. Roberts, and X. Tang, *Nuclear Instruments and Methods in Physics Research Section A: Accelerators, Spectrometers, Detectors and Associated Equipment* **880**, 162846 (2018).
 [18] Y. Giomataris, P. Rebourgeard, J. Robert, and G. Charpak, *Nuclear Instruments and Methods in Physics Research Section A: Accelerators, Spectrometers, Detectors and Associated Equipment* **386**, 1 (1997).
 [19] M. Cortesi, S. Rost, W. Mittig, Y. Ayyad-Limonge, D. Bazin, J. Yurkon, and A. Stolz, *Review of Scientific Instruments* **88**, 013303 (2017), <https://doi.org/10.1063/1.4974333>.
 [20] C. Dalitz, Y. Ayyad, J. Wilberg, L. Aymans, D. Bazin, and W. Mittig, *Computer Physics Communications* **235**, 159 (2019).
 [21] J. Bradt, D. Bazin, F. Abu-Nimeh, T. Ahn, Y. Ayyad, S. B. Novo, L. Carpenter, M. Cortesi, M. Kuchera, W. Lynch, W. Mittig, S. Rost, N. Watwood, and J. Yurkon, *Nuclear Instruments and Methods in Physics Research Section A: Accelerators, Spectrometers, Detectors and Associated Equipment* **880**, 162846 (2018).
 [22] Ayyad, Y., Bazin, D., Beceiro-Novo, S., Cortesi, M., and Mittig, W., *Eur. Phys. J. A* **54**, 181 (2018).
 [23] I. Bylinskii and M. K. Craddock, *Hyperfine Interactions* **225**, 9 (2014).
 [24] J. Lassen, P. Bricault, M. Domsbky, J. P. Lavoie, C. Geppert, and K. Wendt, in *Laser 2004*, edited by Z. Błaszczak, B. Markov, and K. Marinova (Springer Berlin Heidelberg, Berlin, Heidelberg, 2006) pp. 69–75.
 [25] J. F. Ziegler, M. Ziegler, and J. Biersack, *Nuclear Instruments and Methods in Physics Research Section B: Beam Interactions with Matter* **199**, 1 (2003).
 [26] M. S. Hussein, A. F. R. de Toledo Piza, O. K. Vorov, and A. K. Kerman, *Phys. Rev. C* **60**, 064615 (1999).
 [27] A. O. Macchiavelli, H. L. Crawford, C. M. Campbell, R. M. Clark, M. Cromaz, P. Fallon, M. D. Jones, I. Y. Lee, and M. Salathe, *Phys. Rev. C* **97**, 011302 (2018).